Output Feedback Synthesis for a Two-Agent Nonlinear Microrobotic System

Yixin Sun, Matthieu Fruchard, Antoine Ferreira

Output Feedback Synthesis for a Two-Agent Nonlinear Microrobotic System

Yixin Sun[1], Matthieu Fruchard[2], Antoine Ferreira[1]

***Abstract*— Most of minimally invasive therapeutic applications demand to control multiple microrobots. If such microrobots are actuated by a magnetic device whose magnetic field is stationary, like magnetic resonance imaging devices, there is only a single control input per axis so the system is underactuated. Besides, imaging provides only a poor information about the robots state. That is the reason why it is necessary to synthesize observers to rebuild enough information to enable the stabilization of the two-agent system along a reference trajectory. This work addresses the observability and output feedback synthesis for two microrobots facing the blood flow. We propose two observers syntheses depending on the available output of the system: a Luenberger observer if the imaging provides the position of each robot, and a high gain observer if magnetic artifacts only allow for a measurement of a single linear combination of the robots positions. The output feedback is then designed using an exact feedback linearization approach. Simulations illustrate the efficiency of the proposed approach for both observers.**

I. Introduction

There is an ongoing interest for the control of therapeutic microrobots because they are promising to perform minimally invasive surgery and *in situ* diagnosis with lessened side effects. To avoid an embedded energy payload and to optimize the payload ratio, deported magnetic actuation has been widely approved [1]. Such robots design depends on the magnetic actuator properties: elastic flagellated microrobots [2], [3] and helical tail robots [4], [5] require an oscillating magnetic field, and bead pulled robots [6], [7] require a magnetic gradients generation. Controllability [8] and observability [9] for a single agent have been addressed quite recently. [10], [11] and [12] have proposed nonlinear approaches to feedback and output feedback stabilize one microrobot along a reference trajectory. However a single agent may not be sufficient to perform *e.g.* drug targeting or simultaneous sensing and surgical intervention, whence the interest in controlling a multi-agent microrobotic system. A first obstruction to the control of multiple microrobots is the underactuation of the system since independent control of p degrees of freedom for n agents requires np coils [13]. To circumvent this issue, the authors in [14], [15] proposed to exploit the natural frequency differences between the robots to actuate one or part of them with a point to point control objective. Since the controllability of a magnetic gradient actuated system with stationary magnetic field requires to consider the magnetic interaction between nearby agents, [16] and [17] exploited this interaction to perform respectively a relative position and a trajectory tracking objective. Another obstruction is the insufficient imaging resolution. In most works, the system full state [17] or at least the positions of each agent [15], [16], [13], [18] are supposed to be accessible to the measurement. In [13], [18], the authors developed linear state observers to rebuild the agents velocities and thence addressed linear output feedbacks. However, the magnetic interaction between microrobots operating in close vicinity is a nonlinear force, so there is a need to develop tools for the observation of such nonlinear systems if the robots velocities are not measured. Besides if susceptibility artifacts can be helpful to localize microrobots whose size is lower than the imager resolution [19], they can also be detrimental to the simultaneous localization of each robot. In such a case, the imager can only provide a measurement of a single linear combination of the robots positions.

In this paper, we address the output feedback synthesis for two magnetic microrobots facing a pulsatile blood flow with the objective of stabilizing their positions and velocities along an admissible trajectory with a single control input, should both positions or only a linear combination of them be measured. Section II is devoted to a brief recall of the nonlinear dynamics of a two-agent microrobotic system. We then give some necessary conditions for the controllability and observability of such a nonlinear system in Section III. This first contribution is then exploited in Section IV where we propose *i)* a Luenberger observer if each microrobot position can be measured, *ii)* an high gain observer should the imager only provide one output which is an image of the robots positions, and *iii)* an exact feedback linearization approach to stabilize the system along an admissible trajectory using the estimated state. Simulation results illustrate the two proposed output feedbacks in Section V and the results are discussed in Section VI.

II. Modeling

The two agents R_1 and R_2 are spherical microrobots or aggregates facing the blood flow in the arterial network, depicted in the Figure 1, whose positions are denoted x_1 and x_2 respectively along the $\vec{\imath}$ axis. Each microrobot is affected by the drag force $\vec{F}_d$, the motive magnetic force $\vec{F}_m$ and the magnetic interaction $\vec{F}_{kj}$ between robots R_j and R_k, so the equation of motion for the microrobot R_j is given as follows:

$$m_j \ddot{x}_j \vec{\imath} = \vec{F}_{m_j} + \vec{F}_{d_j} + \vec{F}_{kj} \tag{1}$$

[1] Y. Sun and A. Ferreira are with the Insa-Cvl, Univ. Orléans, Laboratory PRISME, EA 4229, $F18020$, Bourges, France. yixin.sun1@insa-cvl.fr, antoine.ferreira@insa-cvl.fr

[2] M. Fruchard is with the Univ. Orléans, Insa-Cvl, Laboratory PRISME, EA 4229, $F45072$, Orléans, France. matthieu.fruchard@univ-orleans.fr

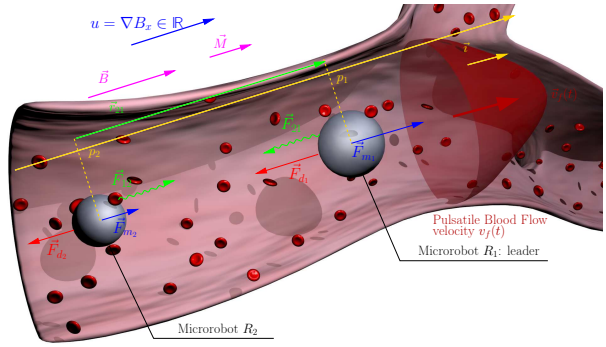

Fig. 1. Forces exerting on two magnetic microrobots R_1 and R_2 in magnetic interaction within a blood vessel: $\vec{F}_{d_j}$, $\vec{F}_{m_j}$, and $\vec{F}_{kj}$ respectively denote the drag force, the magnetic motive force, and the magnetic force interaction that the robot R_k exerts on the microrobot R_j.

where m_j is the mass of robot R_j. For the sake of simplicity, we assume that the spherical micro-agents swim at low Reynolds[1] so the drag force is:

$$\vec{F}_{d_j} = -m_j d_j (\dot{x}_j - v_f(t))\,\vec{i} \qquad d_j = \frac{9\eta}{2\beta_j \rho_j r_j^2} \tag{2}$$

where β_j is a ratio related to the wall effect caused by the partial vessel occlusion by the robot [21], and $v_f(t)$ denotes the pulsatile blood velocity. η, r_j and ρ_j denote respectively the blood viscosity and the microrobot R_j radius and density.

The magnetic motive force for bead pulled magnetic microrobots is given by [20]:

$$\vec{F}_{m_j} = m_j \alpha_j u\,\vec{i} \qquad \alpha_j = \frac{\tau_{m_j} M}{\rho_j} \tag{3}$$

where the control input u is the magnetic field gradient ∇B_x. The robot magnetization and ferromagnetic ratio are denoted $\vec{M}$ and τ_{m_j} respectively, and $M = \|\vec{M}\|$.

A micro-agent R_j with magnetic embedded material has a magnetic moment $\vec{\mathcal{M}}_j = \frac{4}{3}\pi\tau_{m_j} r_j^3 \vec{M}$. Let μ_0 denote the vacuum permeability and $\vec{r}_{kj} = -\vec{r}_{jk} = |p_k - p_j|\vec{\imath}$. Since the magnetic field is stationary $\vec{B} = B_0\vec{\imath}$, the interaction magnetic force [22] exerted by agent R_k on agent R_j is

$$\vec{F}_{kj} = -m_j i_j \frac{\vec{r}_{kj}}{\|\vec{r}_{kj}\|^5}, \quad i_j = \frac{3\mu_0 \mathcal{M}_1 \mathcal{M}_2}{2\pi m_j} \tag{4}$$

Let $x^T = \begin{pmatrix} x_1 & x_2 & \dot{x}_1 & \dot{x}_2 \end{pmatrix} \in \mathcal{X}^+ \cup \mathcal{X}^-$ denote the state vector with $\mathcal{X}^+ = \{x \in \mathbb{R}^4 : x_1 - x_2 > 0\}$ and $\mathcal{X}^- = \{x \in \mathbb{R}^4 : x_1 - x_2 < 0\}$ depending on the relative initial positions. Using (2), (3) and (4) into (1), we obtain the forthcoming nonlinear state space representation:

$$(\mathcal{S}_x) : \begin{cases} \dot{x}_1 &= x_3 \\ \dot{x}_2 &= x_4 \\ \dot{x}_3 &= -d_1(x_3 - v_f) - \frac{i_1}{(x_1 - x_2)^4} + \alpha_1 u \\ \dot{x}_4 &= -d_2(x_4 - v_f) + \frac{i_2}{(x_1 - x_2)^4} + \alpha_2 u \end{cases} \tag{5}$$

Remark 1 *$(\mathcal{S}_x)$ is undefined at $x_1 = x_2$, which explains why the state vector is defined either on $\mathcal{X}^+$ or on $\mathcal{X}^-$. Even if the contact force has not been modeled here, it is physically impossible for the robots to stand at the same location: either R_1 precedes R_2 ($x \in \mathcal{X}^+$), or it is the opposite ($x \in \mathcal{X}^-$), yet the robots can not overtake one another.*

$\forall x_r \in \mathcal{C}^1(\mathbb{R}_+, \mathbb{R}^4), \exists d \in \mathcal{C}^2(\mathbb{R}_+, \mathcal{D})$ with $\mathcal{D} \subset \mathbb{R} \setminus \{0\}$: $d(t) = x_{r1}(t) - x_{r2}(t)$. If the trajectory $x_r(t)$ is admissible, there exists a reference input $u_r(t)$ such that (x_r, u_r) is solution of (5). Let $\tilde{x} = x - x_r \in \tilde{\mathcal{X}}^+ \cup \tilde{\mathcal{X}}^-$, the error system is then an affine nonlinear control system with drift:

$$(\mathcal{S}_{\tilde{x}}) : \begin{cases} \dot{\tilde{x}} = f(\tilde{x}) + g\tilde{u} & \text{(6a)} \\ f(\tilde{x}) = \begin{pmatrix} \tilde{x}_3 \\ \tilde{x}_4 \\ -d_1\tilde{x}_3 - i_1\delta(\tilde{x}) \\ -d_2\tilde{x}_4 + i_2\delta(\tilde{x}) \end{pmatrix}, g = \begin{pmatrix} 0 \\ 0 \\ \alpha_1 \\ \alpha_2 \end{pmatrix} & \text{(6b)} \end{cases}$$

with $\tilde{u} = u - u_r(t)$, $\tilde{\mathcal{X}}^+ = \{\tilde{x} \in \mathbb{R}^4 : \tilde{x}_1 - \tilde{x}_2 + d(t) > 0\}$, $\tilde{\mathcal{X}}^- = \{\tilde{x} \in \mathbb{R}^4 : \tilde{x}_1 - \tilde{x}_2 + d(t) < 0\}$, and the nonlinear function δ defined by

$$\delta : \tilde{x}_1, \tilde{x}_2 \mapsto \frac{1}{(\tilde{x}_1 - \tilde{x}_2 + d(t))^4} - \frac{1}{d^4(t)}. \tag{7}$$

The control objective is to stabilize the error system (6) at zero, using the available system outputs.

III. System Analysis

To our best knowledge, there is currently neither true controllability nor observability study for such nonlinear multi-microagents systems, so we first state on sufficient and necessary conditions for these properties [23].

Lemma 1 *System $(\mathcal{S}_{\tilde{x}})$ is strongly accessible and small-time controllable around $\tilde{x} = 0$ if and only if both following conditions are satisfied:*

- ***C1*** *There exists a magnetic interaction between the robots: $(i_1, i_2) \neq (0, 0)$.*
- ***C2*** *The microrobots parameters $(\alpha_1, \alpha_2, d_1, d_2, i_1, i_2)$ and the planned distance $d(t)$ satisfy:*

$$\frac{4(\alpha_2 - \alpha_1)^2(\alpha_1 i_2 + \alpha_2 i_1)}{\alpha_1 \alpha_2 d(t)^5} \neq (d_2 - d_1)(d_1\alpha_2 - d_2\alpha_1) \tag{8}$$

Controllability is not the core of the paper so we just give here a sketch of proof for this lemma. It is not difficult to show that condition (**C1**) is necessary using Kalman rank condition since the system is linear for $i_1 = i_2 = 0$. The remains of the proof involve Lie bracketing of the control and drift vector fields to check the Lie algebra rank condition.

Lemma 2 *If $y = h(\tilde{x}_1, \tilde{x}_2) \in \mathbb{R}^2$ with $\frac{\partial h}{\partial \tilde{x}}$ full ranked, the system $(\mathcal{S}_{\tilde{x}})$ is locally weakly uniformly observable.*

Lemma 3 *If $y = \mu\tilde{x}_1 + \nu\tilde{x}_2 \in \mathbb{R}$, the system $(\mathcal{S}_{\tilde{x}})$ is locally weakly uniformly observable at any point provided that:*

$$\begin{cases} \mu + \nu \neq 0 & \text{(9a)} \\ \mu\nu(d_1 - d_2)\big(\varphi(d_1 + d_2) + \psi\big) + (\mu + \nu)\varphi^2 \neq 0 & \text{(9b)} \end{cases}$$

where $\varphi = a\delta_1$, $\psi = a(\tilde{x}_3 - \tilde{x}_4)\delta_2 + b\delta_1$ with $a = \nu i_2 - \mu i_1$, $b = \mu d_1 i_1 - \nu d_2 i_2$ and notation $\delta_i(\tilde{x}) = \frac{\partial^i \delta}{\partial \tilde{x}_1^i}(\tilde{x})$.

[1] Yet there is no obstruction to consider nonlinear drag force and non-Newtonian blood modeling, as *e.g.* in [20], [10].

In particular, system $(\mathcal{S}_{\tilde{x}})$ is observable around $\tilde{x}=0$ as soon as the the distance function d is chosen so that

$$d^5 \neq -\frac{4a^2(\nu+\mu)}{\nu\mu(d_1-d_2)(b+a(d_1+d_2))} \tag{10}$$

The proofs of Lemmas 2 and 3 are given in Appendices I and II, respectively.

Remark 2 *The property* (10) *of Lemma 3 ensures that the observability around $\tilde{x}=0$ can always be guaranteed since $d(t)$ is a degree of freedom in the choice of the trajectory.*

Remark 3 *If $d_1=d_2$, then condition* (9) *reduces to $a(\mu+nu)\delta_1\neq 0$. Since $\delta_1\neq 0$ on any compact of $\tilde{\mathcal{X}}$, the uniform observability at any point is guaranteed as soon as $a\neq 0$ and* (9a) *are satisfied.*

IV. Output feedback

We now propose two syntheses of observers for the nonlinear system $(\mathcal{S}_{\tilde{x}})$ depending on the available outputs. First, if both robots positions are measured, system $(\mathcal{S}_{\tilde{x}})$ is linear with an output injection so we propose to use a Luenberger observer for its simplicity. Second, if there is only access to a linear combination of the robots positions, the Luenberger observer is no more useful and we synthesize an high gain observer to rebuild the full state. Then we propose an exact feedback linearization process to ensure the Lyapunov stability of the output feedback. To simplify the study, we consider in this section the case where the microrobotic system design is such that $d_1=d_2$.

A. Luenberger Observer

Proposition 1 *Under the assumptions of Lemma 2, we have access to an output $y=h(\tilde{x})=C\tilde{x}\in\mathbb{R}^2$ with $C=\begin{pmatrix}C_1 & O_2\end{pmatrix}$ and C_1 is invertible. Then*

$$\dot{\zeta}=A\zeta+\phi(y)+g\tilde{u}+L(y-C\zeta) \tag{11}$$

with $A=\begin{pmatrix}0_2 & I_2\\ 0_2 & -D\end{pmatrix}, D=\begin{pmatrix}d_1 & 0\\ 0 & d_2\end{pmatrix}$, *and*

$$\phi^T(y)=\begin{pmatrix}0 & 0 & -i_1 & i_2\end{pmatrix}\delta(C_1^{-1}y) \tag{12}$$

and a gain L such that the matrix $A-LC$ is Hurwitz, is a Luenberger observer of system $(\mathcal{S}_{\tilde{x}})$.

Proof: Using $y=\begin{pmatrix}C_1 & O_2\end{pmatrix}\tilde{x}$ gives $(\tilde{x}_1\ \tilde{x}_2)^T=C_1^{-1}y$ since C_1 is invertible by assumption in Lemma 2. Since the δ function given by (7) only depends on $(\tilde{x}_1-\tilde{x}_2)$, δ can be rewritten as a function of the output y. It follows that system $(\mathcal{S}_{\tilde{x}})$ is linear up to an output injection:

$$\dot{\tilde{x}}=A\tilde{x}+\phi(y)+g\tilde{u} \tag{13}$$

with the matrix A and the vector valued function ϕ given by (12) and the control vector field g given by (6b). Let $\varepsilon=\tilde{x}-\zeta$ denote the observation error. Then, using (11)-(13), the error dynamics are given by $\dot{\varepsilon}=(A-LC)\varepsilon$. Let $L^T=\begin{pmatrix}L_1^T & L_2^T\end{pmatrix}$ with square matrices L_i. It follows that:

$$(A-LC)=\begin{pmatrix}-L_1C_1 & I_2\\ -L_2C_1 & -D\end{pmatrix} \tag{14}$$

For instance let $L_2=0_2$ and choose any Hurwitz 2×2 matrix H. Since C_1 is invertible, it is straightforward that the matrix $(A-LC)$ can be made Hurwitz using $L_1=C_1^{-1}H$. ■

B. High gain observer

Susceptibility artifacts in a magnetic resonance imager is widely used *e.g.* by contrast agents to increase the imager resolution since these artifacts are far bigger than the material. So such a phenomenon can be helpful to localize agents whose size would be smaller than the imager resolution. However, if two agents are in close vicinity, their susceptibility artifacts can overlay, thus resulting in a single artifact. The imager can no more provide the positions of each agent, yet rather a linear combination of their positions, with coefficients related to their magnetic load.

The Luenberger synthesis proposed in Proposition 1 is appealing due to its simplicity, and it would be nice if it could also be applied in the present case. To do so, the system $(\mathcal{S}_{\tilde{x}})$ has to be linear up to an injection term. If the output were $y=\mu(\tilde{x}_1-\tilde{x}_2)$, this condition would be fulfilled. Yet we have proved in Lemma 3 that such an output prevents the system from being observable since condition (9a) is broken. We consequently propose another idea to synthesize the system observer.

Lemma 4 *Let $\mathcal{L}_f^i h$ denote the i-th Lie derivative of h along f and $\delta_i(\tilde{x})=\frac{\partial^i\delta}{\partial\tilde{x}_1^i}(\tilde{x})$. Under the assumptions of Lemma 3, when $d_1=d_2$, the system $(\mathcal{S}_{\tilde{x}})$ is diffeomorphic to*

$$(\mathcal{S}_z):\dot{z}=A_cz+\bar{f}(z)+\bar{g}(z)\tilde{u} \tag{15}$$

with $z=\phi(\tilde{x})$ given by $z_1=y=h(\tilde{x})$, $z_{i+1}=\mathcal{L}_f^i h(\tilde{x})$, A_c a matrix whose non null entries is a unitary superdiagonal, and functions $\bar{f}$, $\bar{g}$ whose non null entries are:

$$\begin{aligned}
&\bar{f}_4: z\mapsto -d_1^3(\mu\tilde{x}_3-\nu\tilde{x}_4)+a\delta_2(\tilde{x}_4-\tilde{x}_3)^2\\
&\qquad -2ad_1\delta_1(\tilde{x}_4-\tilde{x}_3)+\delta[ad_1^2-(i_1+i_2)a\delta_1]\\
&\bar{g}_2: z\mapsto \mu\alpha_1+\nu\alpha_2, \qquad \bar{g}_3: z\mapsto -d_1\bar{g}_2\\
&\bar{g}_4: z\mapsto d_1^2\bar{g}_2+(\alpha_1-\alpha_2)a\delta_1
\end{aligned} \tag{16}$$

The proof of this lemma is given in Appendix III.

Proposition 2 *Under the assumptions of Lemma 4, we have access to an output $y=h(\tilde{x})=C\tilde{x}\in\mathbb{R}$ with $C=\begin{pmatrix}\mu & \nu & 0 & 0\end{pmatrix}$ satisfying condition* (9). *Then let $C_z=\begin{pmatrix}1 & 0 & 0 & 0\end{pmatrix}$, $\bar{f}_{4s}$ and $\bar{g}_{4s}$ denote saturated functions of $\bar{f}_4$ and $\bar{g}_4$ on a given compact included in either $\tilde{\mathcal{X}}^+$ or $\tilde{\mathcal{X}}^-$, G be a gain vector chosen so that A_c-GC_z is Hurwitz. Then, there exists a gain $\theta>0$ such that*

$$\dot{\zeta}=f(\zeta)+g\tilde{u}+\frac{\partial\phi}{\partial\tilde{x}}\Delta_\theta G(y-C\zeta) \tag{17}$$

is an high gain observer of system $(\mathcal{S}_{\tilde{x}})$ in the $\tilde{x}$ coordinates, with Δ_θ is formed in ascending powers of θ.

Proof: System $(\mathcal{S}_z)$ is on an observability normal form with an output $y=C_zz$. Besides, on any compact set in either $\tilde{\mathcal{X}}^+$ or $\tilde{\mathcal{X}}^-$, the function $\bar{f}(z)+\bar{g}(z)\tilde{u}$ can made

globally Lipschitz with respect to z and uniformly with respect to $\tilde{u}$ using bounded extensions $\bar{f}_s$ and $\bar{g}_s$ outside the compact since the control input is bounded. So $(\mathcal{S}_z)$ admits an high gain observer [24] in the following form:

$$\dot{\hat{z}} = A_c\hat{z} + \bar{f}_s(\hat{z}) + \bar{g} - s(\hat{z})\tilde{u} + \Delta_\theta G(y - C_z\hat{z}) \qquad (18)$$

with the diagonal matrix Δ_θ whose diagonal entries are $\Delta_{\theta,i} = \theta^i$ for a given $\theta > \theta_0$ with θ_0 related to the Lipschitz constant of $\bar{f}_s(z) + \bar{g}_s(z)\tilde{u}$, and a gain G chosen so that $A_c - GC_z$ is Hurwitz. So the z observation error $\varepsilon_z = z - \hat{z}$ is stabilized to zero with an arbitrarily fast convergence rate.

One could have then used $\hat{x} = \phi^{-1}(\hat{z})$ as an observer for system $(\mathcal{S}_{\tilde{x}})$, yet the inversion of ϕ is difficult because ϕ is a nonlinear mapping (terms in δ_i in the two last equations of (A.28)). That is the reason why we propose an observer in the natural coordinates $\tilde{x}$.

From Lemma 4, since ϕ is a diffeomorphism, we have $\dot{z} = \frac{\partial\phi}{\partial\tilde{x}}\dot{\tilde{x}}$. Rewritting the z dynamics (15) as $\dot{z} = \omega(z, \tilde{u})$ and using (6), we conclude that

$$\dot{\tilde{x}} = \Big(\frac{\partial\phi}{\partial\tilde{x}}\Big)^{-1}\omega(z, \tilde{u}) = f(\tilde{x}) + g\tilde{u} \qquad (19)$$

The observer (18) in the z coordinates can be rewritten as:

$$\dot{\hat{z}} = \omega(\hat{z}, \tilde{u}) + \Delta_\theta G(y - C_z\hat{z}) \qquad (20)$$

It follows that the observer in the $\tilde{x}$ coordinates is given by:

$$\dot{\zeta} = \Big(\frac{\partial\phi}{\partial\tilde{x}}\Big)^{-1}\Big(\frac{\partial\phi}{\partial\tilde{x}}(f(\zeta) + g\tilde{u}) + \Delta_\theta G(y - C_z\hat{z})\Big) \qquad (21)$$

Finally, using $C_z\hat{z} = \mu\zeta_1 + \nu\zeta_2$, (17) is an high gain observer of $(\mathcal{S}_{\tilde{x}})$ in the $\tilde{x}$ coordinates. ∎

C. Controller

The controller design relies on exact feedback linearization. We first use a technical lemma to map $(\mathcal{S}_{\tilde{x}})$ to a pure feedback form, and then derive a linearizing control law to stabilize the image state to zero, implying the stabilization of state $\tilde{x}$ to zero.

Lemma 5 *Under assumptions of Lemmas 1 and 4, when $d_1 = d_2$, the system $(\mathcal{S}_{\tilde{x}})$ is diffeomorphic to*

$$(\mathcal{S}_s) : \begin{cases} \dot{s}_1 &= s_2 \\ \dot{s}_2 &= s_3 \\ \dot{s}_3 &= s_4 \\ \dot{s}_4 &= \bar{\bar{f}}_4(s) + \bar{\bar{g}}_4\tilde{u} \end{cases} \qquad (22)$$

with $s = \bar{\phi}(\tilde{x})$ given by $s_1 = \alpha_2\tilde{x}_1 - \alpha_1\tilde{x}_2 = \bar{h}(\tilde{x})$, and $s_{i+1} = \mathcal{L}^i_{\bar{f}}\bar{h}(\tilde{x})$, $i = 1, \ldots, 3$. Let $p = \alpha_2 i_1 + \alpha_1 i_2$, the functions $\bar{\bar{f}}$, $\bar{\bar{g}}$ only non null entries are:

$$\begin{aligned} \bar{\bar{f}}_4 &: s \mapsto -p\big((d_1(\tilde{x}_4 - \tilde{x}_3) - (i_1 + i_2)\delta)\delta_1 \\ &\qquad + (\tilde{x}_3 - \tilde{x}_4)^2\delta_2\big) - d_1 s_4 \\ \bar{\bar{g}}_4 &: s \mapsto -p(\alpha_1 - \alpha_2)\delta_1 \end{aligned} \qquad (23)$$

Proof: The proof of this lemma is similar to the one of Lemma 4. Under assumption of Lemma 1, when $d_1 = d_2$, the system is controllable provided that $(i_1, i_2, \alpha_1 - \alpha_2) \neq 0$. In such a case, apply Lemma 4 using $\mu = \alpha_2, \nu = -\alpha_1$. Then it is straightforward that (16) gives (23). $\bar{\phi}$ is a diffeomorphism since it is a $\mathcal{C}^1$ mapping and its jacobian is given by:

$$\det\frac{\partial\bar{\phi}}{\partial\tilde{x}} = -(\alpha_1 - \alpha_2)^2(\alpha_2 i_1 + \alpha_1 i_2)\delta_1^2(\tilde{x}) \neq 0 \qquad (24)$$

since $\alpha_1 - \alpha_2 \neq 0$ by Lemma 1, $\alpha_2 i_1 + \alpha_1 i_2 > 0$ and δ_1 does not vanish on any compact. ∎

Proposition 3 *Let $x_r(t), u_r(t)$ denote any admissible $\mathcal{C}^1$ trajectory and the associated reference control input. Under assumptions of Lemma 5, the state feedback*

$$u = \kappa(\tilde{x}) = u_r(t) - \bar{\bar{g}}_4^{-1}(\bar{\bar{f}}_4 + K\bar{\phi}(\tilde{x})) \qquad (25)$$

ensures the semiglobal exponential asymptotic stability of the origin of the system $(\mathcal{S}_{\tilde{x}})$ for any initial bounded state $\tilde{x}(0)$ lying in either $\tilde{\mathcal{X}}^+$ or $\tilde{\mathcal{X}}^-$ for some positive gain K such that $(A_c - \bar{\bar{g}}K)$ is Hurwitz. Then the output feedback

$$u = \kappa_s(\zeta) \qquad (26)$$

semiglobally stabilizes the origin of the system $(\mathcal{S}_{\tilde{x}})$ for θ large enough in Proposition 2 if ζ is given by (17)*, or poles placed left enough in Proposition 1 if ζ is given by* (11)*, with κ_s a bounded extension of the κ function in* (25)*.*

Proof: The proof relies on [25]: peaking phenomenon and possible escape in finite time are circumvented using the saturation extensions of functions f, g and κ. ∎

V. Simulations

TABLE I
PARAMETERS VALUES FOR BOTH SIMULATIONS

Parameter [unit]	Symbol	Values	
Magnetization $[A\ m^{-1}]$	M	$1.72\ 10^6$	
Robots radius $[m]$	r_1, r_2	$200\ 10^{-6}$	$200\ 10^{-6}$
Robots density $[kg\ m^{-3}]$	ρ_1, ρ_2	6873	6873
Ferromagnetic ratio	τ_1, τ_2	0.85	0.025
Wall effect ratio	β_1, β_2	0.724	0.724
Control parameter $[A\ m^2\ s^{-2}]$	α_1, α_2	212.72	6.25
Drag parameter $[s^{-1}]$	d_1, d_2	474.6	474.6
Interaction parameter $[m^5\ s^{-2}]$	i_1, i_2	$1.84\ 10^{-10}$	$1.84\ 10^{-10}$

TABLE II
PHYSIOLOGICAL VALUES FOR BOTH SIMULATIONS

Parameter [unit]	Symbol	Value
Blood viscosity $[Pa\ s]$	η	$21\ 10^{-3}$
Vessel radius $[m]$	R	$1.5\ 10^{-3}$
Mean blood velocity $[m\ s^{-1}]$	a_0	$-25\ 10^{-3}$
Amplitude of the blood pulse $[m\ s^{-1}]$	a_1	$9\ 10^{-3}$

We consider two microagents R_1 and R_2 whose parameters are given in Table I. The first simulation illustrates the case where the positions of both microrobots are measured: $y = (\tilde{x}_1\ \ \tilde{x}_2)^T$, whilst the second one illustrates the case

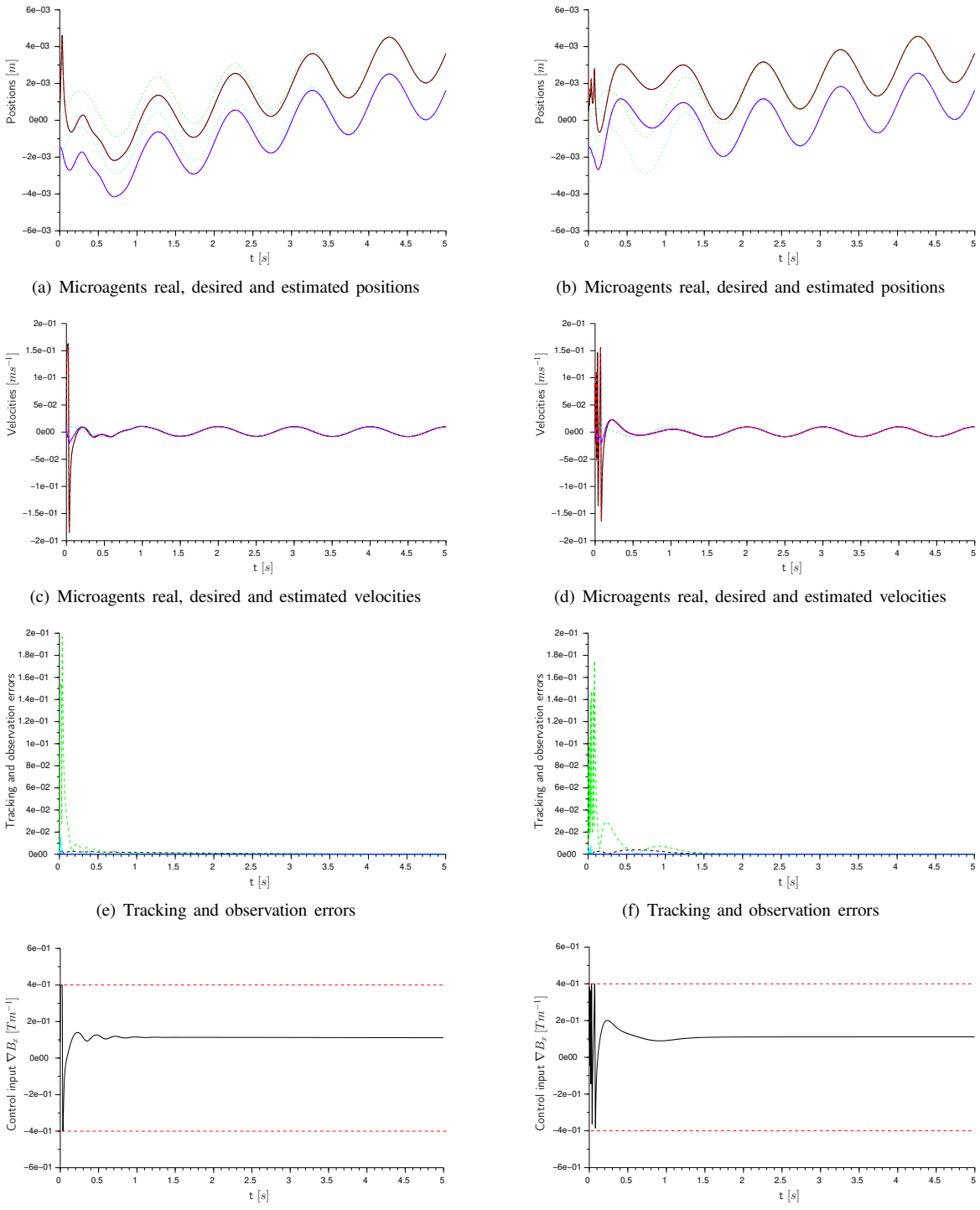

(a) Microagents real, desired and estimated positions

(b) Microagents real, desired and estimated positions

(c) Microagents real, desired and estimated velocities

(d) Microagents real, desired and estimated velocities

(e) Tracking and observation errors

(f) Tracking and observation errors

(g) Control input

(h) Control input

Fig. 2. From left to right: simulation when 2 outputs are available and simulation when only a single output is available. From top to bottom: (a)-(b) microagents R_1 and R_2 positions x_1 and x_2 (real: black and blue solid lines, desired: green and cyan dots, estimated: red and purple dashes), (c)-(d) microagents R_1 and R_2 velocities x_3 and x_4 (real: black and blue solid lines, desired: green and cyan dots, estimated: red and purple dashes), (e)-(f) microagents R_1 and R_2 tracking (position: black dashes, velocity: green dashes) and observation norms (position: blue line, velocity: cyan line), and (g)-(h) the control input of the system with saturations $\pm u_{sat}$ depicted in red dashes.

where the output is a linear combination of the agents positions: $y = \alpha_2 \tilde{x}_1 - \alpha_1 \tilde{x}_2$. The parameters are such that the system is controllable according to Proposition 1, and observable according to Lemmas 2 and 3 for $d_1 = d_2$. The initial conditions are given by

$$x_0 = \begin{pmatrix} 0.0005 & -0.0025 & 0 & 0 \end{pmatrix}^T$$
$$x_{r0} = \begin{pmatrix} 0 & -0.002 & 0 & 0 \end{pmatrix}^T$$
$$\zeta_0 = \tilde{x}_0 + \begin{pmatrix} 0.0005 & 0 & 0.0005 & 0.0005 \end{pmatrix}^T$$

The pulsatile blood velocity is modeled by the Womersley model [26] approximation. To be consistent with the vessel radius and to simplify the study, we have chosen a first-order truncated Fourier series $v_f(t) = a_0 + a_1 \cos 2\pi t$ with a negative mean value so that the microrobots swim against the flow. Physiological data are given in Table II.

The output feedback is given by (26) with a gain $K = \begin{pmatrix} 40 & 20 & 40 & 10 \end{pmatrix}$ and the reference trajectory is chosen so as $d = 2mm$. This reference is admissible for the underactuated system, yet since the microagents are not at the right initial state, they have to recover this trajectory while satisfying the underactuation constraints. The control input is saturated using $u_a(t) = u(t)/k(t)$ with $k(t) = \max\left(1, |u(t)|/u_{sat}\right)$ and $u_{sat} = 0.4Tm^{-1}$.

A. Microagents positions are both measured

This first simulation illustrates the output feedback results when using the Luenberger observer given by Proposition 1 with the gain matrix $L^T = \begin{pmatrix} L_1^T & L_2^T \end{pmatrix}$ where $L_1 = 100I_2$ and $L_2 = 0_2$. The simulation results are depicted in the left column of Figure 2. Figures 2(a) and 2(c) illustrate the convergence of the two agents estimates to the nominal state within a very short $0.05s$ transient phase. Such a behavior was expected since the stability of the two last components of the state is driven by the values of $-d_1$ and $-d_2$ (see (14)), meaning that the poles are placed far left. These figures also illustrate the slower convergence of the position and velocity tracking to their references, see also Figure 2(e), after a $3s$ period once the observer error has converged. At the simulation beginning, the tracking and observation errors are high, so that the control input on Figure 2(g) takes high values and thus reaches both lower and upper saturations. The system errors depicted on Figure 2(e) are then stabilized to zero.

B. The output is only a linear combination of the agents positions

This second simulation is led while the only output of the system is an image of both robots positions. In such a case, it is impossible to use the Luenberger observer, and the high gain observer synthesized in Proposition 2 is used instead. The high gain parameters are $\theta = 8$ and a gain G given by

$$G = \begin{pmatrix} 40 & 600 & 8.43 & 21.10 \end{pmatrix}^T \tag{27}$$

The choice of a quite high θ is constrained by the high Lipschitz constant of the system on the set where no saturation is imposed. Consequently, the convergence of the high gain observer is also fast, around $0.1s$ as it can be noticed on Figures 2(b)-2(d). Since we have access to less information, the behavior of the controlled system is impacted: the initial tracking is more degraded here than in the first simulation.

This is due to the fact that the microagents system is very sensitive to the nonlinear term δ that depends on the inverse fourth power of the relative robots position, which is not measured: a small error on this relative distance causes high accelerations -hence the high Lipschitz constant of the system. The control input, plotted on Figure 2(h), behaves like a bang-bang controller at the beginning, and the velocities observation error is relatively high because we are more interested in a fast convergence of the positions observation error to reduce the impact of the nonlinear term. Ironically, the tracking objective is reached faster than in the first simulation, around $2s$, because the resulting state after the observer convergence is more favorable to the underactuated system constraints.

VI. Discussion and conclusion

In this paper, we have proposed a stabilizing output feedback for a two-agent underactuated microrobotic system when imaging modalities may imply some loss of information that has not yet been considered in the literature. First, we have proposed a nonlinear observability analysis both in the case where it is possible to measure each agent position and in the case where susceptibility artifacts jeopardize this assumption so that only a single information about the positions is measured. In each case, a nonlinear state observer has been proposed to rebuild the missing information, which is required for a trajectory tracking objective. Lastly, output feedbacks have been synthesized to stabilize the system along any reference admissible trajectory.

Further perspectives and on-going works include the robustness of the proposed approach to both output noise and parametric uncertainties that are inherent to the microworld and biophysical systems, respectively. For instance, we have supposed that the blood velocity was known whilst it is likely that such an information is hardly accessible with enough spatial and temporal resolution. On going work is thus led to generalize the state estimation approach previously developed in [12] for a single microrobot. Another perspective is the extension of this approach to more agents.

Appendix I
Proof of Lemma 2

Let $\mathcal{O}$ denote the smallest vector space that contains h and closed under the Lie derivative $\mathcal{L}_\tau$, where $\tau \in \{f, g\}$, *i.e.* such that $\forall \sigma \in \mathcal{O}$, $\mathcal{L}_\tau(\sigma) \in \mathcal{O}$. $\mathcal{O}$ is called the observation set. Now $\mathrm{d}\mathcal{O} = Span\{\mathrm{d}\tau, \tau \in \mathcal{O}\}$ is the observability co-distribution. A system is weakly observable if $\dim \mathrm{d}\mathcal{O} = \dim \tilde{\mathcal{X}}$. If $y = h(\tilde{x}_1, \tilde{x}_2)$ with $C_1 = \frac{\partial h}{\partial \tilde{x}}$ full ranked, it is not difficult to show using (6b), that

$$\begin{aligned} \mathrm{d}\mathcal{O} &= Span\{\mathrm{d}h_1, \mathrm{d}h_2, \mathrm{d}\mathcal{L}_f h_1, \mathrm{d}\mathcal{L}_f h_2\} \\ &= Span\{\begin{pmatrix} C_1 & O_2 \\ * & C_1 \end{pmatrix}\} \end{aligned}$$

with $C_1 = \begin{pmatrix} \frac{\partial h}{\partial \tilde{x}_1} & \frac{\partial h}{\partial \tilde{x}_2} \end{pmatrix}$. Since C_1 is full rank, it is straightforward that the system is observable.

Appendix II
Proof of Lemma 3

If $y = h(\tilde{x}) = \mu\tilde{x}_1 + \nu\tilde{x}_2$, we compute the successive Lie derivatives:

$$\begin{aligned} \mathcal{L}_f h(\tilde{x}) &= \mu\tilde{x}_3 + \nu\tilde{x}_4 \\ \mathcal{L}_f^2 h(\tilde{x}) &= -\mu d_1 \tilde{x}_3 - \nu d_2 \tilde{x}_4 + a\delta \\ \mathcal{L}_f^3 h(\tilde{x}) &= \mu d_1^2 \tilde{x}_3 + \nu d_2^2 \tilde{x}_4 + a\delta_1(\tilde{x}_3 - \tilde{x}_4) + b\delta \end{aligned} \tag{A.28}$$

with parameters $a = \nu i_2 - \mu i_1$, $b = \mu d_1 i_1 - \nu d_2 i_2$ and function $\delta_i(\tilde{x}) = \frac{\partial^i \delta}{\partial \tilde{x}_1^i}(\tilde{x})$. Hence we get:

$$\begin{array}{rcl} \mathrm{d}h(\tilde{x}) & = & \begin{pmatrix} \mu & \nu & 0 & 0 \end{pmatrix} \\ \mathrm{d}\mathcal{L}_f h(\tilde{x}) & = & \begin{pmatrix} 0 & 0 & \mu & \nu \end{pmatrix} \\ \mathrm{d}\mathcal{L}_f^2 h(\tilde{x}) & = & \begin{pmatrix} a\delta_1 & -a\delta_1 & -\mu d_1 & -\nu d_2 \end{pmatrix} \\ \mathrm{d}\mathcal{L}_f^3 h(\tilde{x}) & = & \begin{pmatrix} a(\tilde{x}_3 - \tilde{x}_4)\delta_2 + b\delta_1 \\ -a(\tilde{x}_3 - \tilde{x}_4)\delta_2 - b\delta_1 \\ \mu d_1^2 + a\delta_1 \\ \nu d_2^2 - a\delta_1 \end{pmatrix}^T \end{array} \quad \text{(A.29)}$$

Using (A.29), we obtain:

$$\det \mathrm{d}\mathcal{O} = -\Big(\mu\nu(d_1 - d_2)\big(\varphi(d_1 + d_2) + \psi\big) + (\mu + \nu)\varphi^2\Big) \\ (\mu + \nu) \quad \text{(A.30)}$$

with $\varphi = a\delta_1$ and $\psi = a(\tilde{x}_3 - \tilde{x}_4)\delta_2 + b\delta_1$. Hence the condition (9). Besides, since $\delta_1 = \frac{-4}{d(t)^5}$ for $\tilde{x} = 0$, we can deduce (10) from (9).

Appendix III
Proof of Lemma 4

Let $z = \phi(\tilde{x})$ given by:

$$\left\{ \begin{array}{rcl} h(\tilde{x}) & = & \alpha_2 \tilde{x}_1 - \alpha_1 \tilde{x}_2 \\ z_{i+1} & = & \mathcal{L}_f^i h(\tilde{x}),\ i = 0, \ldots, 3 \end{array} \right. \quad \text{(A.31)}$$

Using Lie differentiation like in the Appendix II, it is straightforward that ϕ is a local diffeomorphism under assumptions of Lemma 3 since ϕ is $\mathcal{C}^1$ and its jacobian is non singular:

$$\det \frac{\partial \phi}{\partial \tilde{x}} = \det \mathrm{d}\mathcal{O} \neq 0 \quad \text{(A.32)}$$

with (μ, ν) such that $\lambda + \nu \neq 0$ and $a = \nu i_2 - \mu i_1 \neq 0$. Differentiating (A.31) leads to:

$$\left\{ \begin{array}{rcl} \dot{z}_1 & = & z_2 \\ \dot{z}_2 & = & z_3 + \bar{g}_2 \tilde{u} \\ \dot{z}_3 & = & z_4 + \bar{g}_3 \tilde{u} \\ \dot{z}_4 & = & \bar{f}_4(z) + \bar{g}_4 \tilde{u} \end{array} \right. \quad \text{(A.33)}$$

that is system $(\mathcal{S}_z)$ in (15) with A_c a matrix whose non null entries is a unitary superdiagonal and functions $\bar{f}$, $\bar{g}$:

$$\bar{f}(z) = \begin{pmatrix} 0 & 0 & 0 & \bar{f}_4(z) \end{pmatrix}^T,\ \bar{g}(z) = \begin{pmatrix} 0 & \bar{g}_2 & \bar{g}_3 & \bar{g}_4(z) \end{pmatrix}^T$$

with the $\bar{f}_i$, $\bar{g}_i$ given by (16).

References

[1] B. J. Nelson, I. K. Kaliakatsos, and J. J. Abbott, "Microrobots for minimally invasive medecine," *Annual Review of Biomedical Engineering*, vol. 12, pp. 55–85, 2010.

[2] M. C. Lagomarsino, F. Capuani, and C. P. Lowe, "A simulation study of the dynamics of a driven filament in an aristotelian fluid," *Journal of Theoretical Biology*, vol. 224, no. 2, pp. 215–224, 2003.

[3] A. A. Evans and E. Lauga, "Propulsion by passive filaments and active flagella near boundaries," *Physical Review E*, vol. 82, no. 4, pp. 041 915.1–041 915.12, 2010.

[4] R. Dreyfus, J. Beaudry, M. L. Roper, M. Fermigier, H. A. Stone, and J. Bibette, "Microscopic artificial swimmers," *Nature*, vol. 437, pp. 862–865, 2005.

[5] L. Zhang, K. E. Peyer, and B. J. Nelson, "Artificial bacterial flagella for micromanipulation," *Lab on a chip*, vol. 10, no. 17, pp. 2203–2215, 2010.

[6] J. J. Abbott, K. E. Peyer, M. C. Lagomarsino, L. Zhang, L. X. Dong, I. K. Kaliakatsos, and B. J. Nelson, "How should microrobots swim?" *International Journal of Robotics Research*, vol. 28, pp. 1434–1447, 2009.

[7] J.-B. Mathieu, G. Beaudoin, and S. Martel, "Method of propulsion of a ferromagnetic core in the cardiovascular system through magnetic gradients generated by an MRI system," *IEEE Transactions on Biomedical Engineering*, vol. 53, no. 2, pp. 292–299, 2006.

[8] L. Giraldi and J. B. Pomet, "Local controllability of the two-link magneto-elastic micro-swimmer," *IEEE Transactions on Automatic Control*, vol. 62, no. 5, pp. 2512–2518, 2017.

[9] M. Fruchard, L. Arcese, and E. Courtial, "Estimation of the blood velocity for nanorobotics," *IEEE Transactions on Robotics*, vol. 30, no. 1, pp. 93–102, 2014.

[10] L. Arcese, M. Fruchard, and A. Ferreira, "Adaptive controller and observer for a magnetic microrobot," *IEEE Transactions on Robotics*, vol. 29, no. 4, pp. 1060–1067, 2013.

[11] T. Xu, G. Hwang, N. Andreff, and S. Régnier, "Planar path following of 3D steering scaled-up helical microswimmers," *IEEE Transactions on Robotics*, vol. 31, no. 1, pp. 117 – 127, 2015.

[12] L. Sadelli, M. Fruchard, and A. Ferreira, "2D observer-based control of a vascular microrobot," *IEEE Transactions on Automatic Control*, vol. 62, no. 5, pp. 2194–2206, 2017.

[13] A. Denasi and S. Misra, "Independent and leader-follower control for two magnetic micro-agents," vol. 3, pp. 218–225, 1 2018.

[14] S. Floyd, E. Diller, C. Pawashe, and M. Sitti, "Control methodologies for a heterogeneous group of untethered magnetic micro-robots," *International Journal of Robotics Research*, vol. 30, no. 13, pp. 1553–1565, 2011.

[15] E. Diller, S. Floyd, C. Pawashe, and M. Sitti, "Control of multiple heterogeneous magnetic microrobots in two dimensions on nonspecialized surfaces," *IEEE Transactions on Robotics*, vol. 28, no. 1, pp. 172–182, 2012.

[16] M. Salehizadeh and E. Diller, "Two-agent formation control of magnetic microrobots in two dimensions," *Journal of Micro-Bio Robotics*, vol. 12, no. 1, pp. 9–19, 2017.

[17] A. Eqtami and P. E. Dupont, "Stabilizing the relative position of millirobots inside an mri scanner considering magnetic interaction forces," *IEEE International Conference on Intelligent Robots and Systems*, pp. 3220–3226, 2015.

[18] L. Yang, Q. Wang, and L. Zhang, "Model-free trajectory tracking control of two-particle magnetic microrobot," *IEEE Transactions on Nanotechnology*, vol. 17, no. 4, pp. 697–700, July 2018.

[19] T. Wortmann, C. Dahmen, and S. Fatikow, "Study of MRI susceptibility artifacts for nanomedical applications," *Journal of Nanotechnology in Engineering and Medicine*, vol. 1, no. 4, pp. 041 002.1–041 002.5, 2010.

[20] L. Arcese, M. Fruchard, and A. Ferreira, "Endovascular magnetically-guided robots: navigation modeling and optimization," *IEEE Transactions on Biomedical Engineering*, vol. 59, no. 4, pp. 977–987, 2012.

[21] R. Kehlenbeck and R. D. Felice, "Empirical relationships for the terminal settling velocity of spheres in cylindrical columns," *Chemical Eng. Technology*, vol. 21, pp. 303–308, 1999.

[22] P. Vartholomeos and C. Mavroidis, "In silico studies of magnetic microparticle aggregations in fluid environments for MRI-guided drug delivery," *IEEE Transactions on Biomedical Engineering*, vol. 59, no. 11, pp. 3028–3038, 2012.

[23] A. Isidori, *Nonlinear control systems*. Springer-Verlag London, 1995.

[24] J. Gauthier, H. Hammouri, and S. Othman, "A simple observer for nonlinear systems. application to bioreactors." *IEEE Transactions on Automatic Control*, vol. 37(6), pp. 875–880, 1992.

[25] H. Shim and J. H. Seo, "Non-linear output feedback stabilization on a bounded region of attraction," vol. 73, pp. 416–426, 2000.

[26] J. Womersley, "Method for the calculation of velocity, rate of flow and viscous drag in arteries when the pressure gradient is known," *The Journal of physiology*, vol. 127, no. 3, pp. 553–563, 1955.